Interference and SINR in Dense Terahertz Networks

V. Petrov, D. Moltchanov, Y. Koucheryavy
Nano Communications Center
Department of Electronics and Communications Engineering
Tampere University of Technology, Tampere, Finland
Email: vitaly.petrov@tut.fi, dmitri.moltchanov@tut.fi, yk@cs.tut.fi

***Abstract*—Over the last decade short-range communications in the terahertz band have been extensively studied as a technology-enabler for dense and ultra-dense wireless networks. Recent advances in miniaturized terahertz transceivers design promise wireless connectivity and simultaneous interaction between thousands of devices. However, the feasibility of network-wide communications is still an open issue due to specific features of the terahertz band and inherent properties of dense deployments. We address this issue developing an analytical model for interference and SINR assessment in dense terahertz networks obtaining the first two moments and density functions for both metrics. Our results demonstrate that the presence of molecular noise does not qualitatively affect the behavior of SINR, while its quantitative effect is of secondary importance compared to interference. The presented approach provides the so-far missing building block for performance analysis of prospective dense terahertz networks.**

I. Introduction

The terahertz (THz) band, 0.1–10 THz, is a promising frequency range for the next generation ultra-dense wireless networks. Its theoretical channel capacity of few terabits per second [1], [2] is deemed to be sufficient for the broad range of applications, including high-quality video streaming, board-to-board communications and wireless networks on chips.

The size of prospective THz antennas is in the range of several hundreds of micrometers, thus, introducing the communication capabilities to the micro- and nano-scale devices forming the so-called micro- and nanonetworks. These networks are expected to comprise a massive amount of inherently small devices. The functionality of a single node is envisioned to be limited by a set of primitive operations: chemical sensing, data storing, etc. However, by coordination of the nodes activities, nanonetworks can play an important role in such valuable applications as in-body drug delivery, health monitoring and cooperative environmental sensing.

To date, the THz channel properties have been addressed in several studies, starting from the "terahertz pioneer" D. R. Grischkowsky, who has obtained the fundamental trade-offs for the channel [3], and up to J. M. Jornet and I. F. Akyildiz, who have recently investigated the point-to-point communications via this frequency band [1]. At the same time, insufficient effort has been spent so far to analyze the system level performance of the THz networks. This question is of special interest as density of prospective nanonetworks can reach the value of few hundreds of devices per square centimeter [4], while specific properties of THz waves propagation may easily prohibit any communications at this density. To address this issue, an efficient technique to estimate the interference and SINR in a terahertz network is required.

The Signal-to-Interference-plus-Noise Ratio (SINR) is a fundamental metric characterizing the performance of wireless systems. Applying the Shannon's theorem, the SINR can be used to obtain the link capacity in an interference environment. Moreover, the function of SINR degradation with distance determines the effective communication range and the applicability of certain modulation and coding schemes. Surprisingly, to the best of authors' knowledge, no one has yet addressed the question of SINR estimation in THz networks.

In this paper, we develop an analytical framework for SINR estimation in dense THz networks. We first apply the mathematical apparatus of stochastic geometry to get a closed-form equation for the total interference level at the receiver. We then provide an approximation for the SINR value as a function of nodes density and the transmit power. Finally, we study whether the presence of molecular loss and noise qualitatively and/or quantitatively change the SINR behavior.

The rest of the paper is organized as follows. In Section II, we describe the THz channel and noise models. In Section III, we analytically evaluate SINR for a fixed distance between the transmitter and receiver in a field of interferers. In Section IV, we validate our model using simulations and present major numerical trade offs. We conclude the paper in Section V.

II. Terahertz Propagation and Noise Models

There are a number terahertz propagation models proposed to date [1], [2], [3], [5] with [5] being the most applicable to the distances considered in this paper. In this section, we follow [5] to remind the details of the THz propagation complementing it with a more detailed noise model. To describe the THz channel properties, we consider a point-to-point line-of-sight communication scenario of a single transmitter (Tx) and a single receiver (Rx), both with omnidirectional antennas.

The distinguishing feature of the terahertz channel is presence of the molecular absorption loss [1]. This loss is caused by certain type of molecules such as H_20 vapor in the air each having unique absorption spectrum making the wireless channel frequency selective. The link budget equation for the received power spectral density (psd) in the THz band is

$$S_{Rx}(f,d) = \frac{S_{Tx}(f)}{L_A(f,d)L_P(f,d)}, \quad (1)$$

where f is the operating frequency, d is the separation distance between the transmitter and the receiver, $S_{Tx}(f)$ stands for the

978-1-4799-8091-8/15/$31.00 ©2015 IEEE

transmitted signal psd, $L_A(f,d)$ represents the absorption loss, and $L_P(f,d)$ is the propagation loss.

Assuming free space propagation, $L_P(f,d)$ is

$$L_P(f,d) = \left(\frac{4\pi f d}{c}\right)^2, \tag{2}$$

where c is the speed of light.

As stated in [5], the absorption loss is defined as

$$L_A(f,d) = \frac{1}{\tau(f,d)}, \tag{3}$$

where $\tau(f,d)$ is the transmittance of the medium following the Beer-Lambert law, $\tau(f,d) \approx e^{-K(f)d}$, where $K(f)$ is the overall absorption coefficient of the medium available from HITRAN database [6]. Substituting (3) and (2) into (1) we get the received signal psd as

$$S_{Rx}(f,d) = S_{Tx}(f)\frac{c^2}{16\pi^2 f^2} d^{-2} e^{-K(f)d}. \tag{4}$$

To proceed with SINR analysis, in addition to the path loss, we have to specify the noise in THz band. First, absorption of electromagnetic energy by medium results in the so-called molecular noise as molecules re-emit a part of absorbed energy. Following [2], [5], molecular noise psd is given by

$$S_M(f,d) = \frac{S_{Tx}(f)}{L_P(f,d)}[1-\tau(f,d)]. \tag{5}$$

The second part of noise is Johnson-Nyquist noise generated by thermal agitation of electrons in conductors. Notice that if the principal parts of the transceivers are made of superconductive materials, such as graphene, this noise might not be present [7]. If this is not the case, the form of the Johnson-Nyquist noise changes when entering the THz frequencies. The power of this noise stays flat up until 0.1THz at $P_{JN} = k_B T = -174$dBm/Hz, k_B is Boltzmann constant and T is the temperature in Kelvin, and then declines non-linearly up until approximately 6THz where its power becomes zero [8]. In the latter case, following the Plank's law, the Johnson-Nyquist noise becomes a function of the operating frequency. Thus, we approximate its psd using [8]

$$S_{JN}(f) = \frac{hf}{\exp(hf/k_B T) - 1}, \tag{6}$$

where h is Planck's constant.

Summarizing, the total noise psd at the receiver is

$$S_T(f,d) = \frac{hf}{\exp(hf/k_B T) - 1} + \frac{S_{Tx}(f)[1-\tau(f,d)]}{L_P(f,d)}. \tag{7}$$

We heavily rely on (4), (7) in the next section, analyzing the THz network performance.

III. Network Analysis

A. Scenario Definition

We consider a random nodes deployment in $\Re^2$ (see Fig. 1), widely used nowadays for performance assessment of cellular, ad-hoc and device-to-device networks [9]. In particular, we

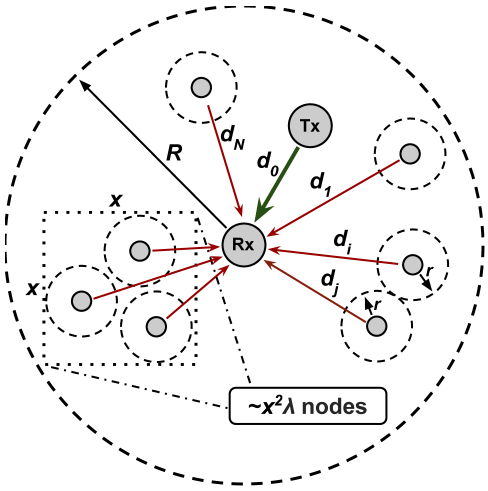

Fig. 1. Considered deployment scenario.

assume the nodes being placed according to isotropic homogenous Mattern hardcore process with intensity λ and parameter r [10], [9], [11]. Recall that this process is a special thinning of the Poisson point process with intensity $\lambda_P > \lambda$ such that the distance between neighbors is at least r. The reason for choosing Mattern process instead of the more studied Poisson point process is that the parameter r allow to reflect the real-life phenomenon, when the distance between two nodes cannot be arbitrarily small. In our scenario r is assumed to be 100 micrometers. The following relation holds between intensities $\lambda_P = (1 - e^{-\lambda P r^2})/r^2\pi$ [10].

A certain node, called a tagged receiver, is chosen as a receiver of interest. Tagged transmitter is placed at a fixed distance, d_0, from the tagged receiver. All the nodes in a point field are considered as interfering nodes for the tagged receiver. In this study, we are particularly interested in SINR metrics, including mean, variance and distribution function at the tagged receiver.

The instantaneous frequency-dependent SINR is defined as:

$$S(\vec{d}, \vec{P}_T, f, \lambda) = \frac{P_{R_0}(d_0, P_T, f, \lambda)}{I(\vec{P}_T, \vec{d}, f, \lambda) + N(\vec{P}_T, \vec{d}, f, \lambda)}, \tag{8}$$

where $P_{R_0}(d_0, P_T, f, \lambda)$ is the received signal power at the separation distance d_0 from the transmitter, $I(\vec{P}_T, \vec{d}, f, \lambda)$ is the aggregate power of the interfering signals at the receiver, $N(\vec{P}_T, \vec{d}, f, \lambda)$ is the noise power at the receiver, $\vec{d}$ is the vector of distances d_i, $i = 1, 2, \ldots, N$, are the separation distances between interferers and the receiver, λ is the intensity of interferers, f is the operating frequency, M is the number of interfering nodes. In this paper we assume no power control capabilities and assign $P_{T_i} = P_{T_j}$, $i, j = 0, 1, \ldots, N$. For simplicity of notation, in what follows, we drop arguments that are often silently assumed, f, P_{T_i} and λ.

The aggregate interference from N sources is given by

$$I(\vec{d}) = \sum_{i=1}^{N} P_{T_i} A_0 d_i^{-2} e^{-K d_i}, \; A_0 = \frac{c^2}{16\pi^2 f^2}. \tag{9}$$

The noise power is written as

$$N(\vec{d}) = N_0 + \sum_{i=1}^{N} P_{T_i} A_0 d_i^{-2}(1 - e^{-Kd_i}), \qquad (10)$$

where $N_0 = k_B T + P_{T_0} A_0 d_0^{-2}(1 - e^{-Kd_0}$.

Substituting (9)-(10) into (9) and simplifying gives

$$S(\vec{d}) = \frac{P_{R_0}}{N_0 + \sum_{i=1}^{N} P_{T_i} A_0 d_i^{-2}}, \qquad (11)$$

where $P_{R_0} = P_{T_0} A_0 d_0^{-2} e^{-Kd_0}$.

B. Methodology Overview

The choice of the Mattern hardcore field makes the analysis complicated. First, the distance to the nth neighbor in a Mattern hardcore process is not known. However, the distance in the Poisson point process with intensity λ used to construct the Mattern process is given by generalized Gamma distribution with integer valued shape parameter [12]. However, as was shown in [10], for small r the Mattern hardcore process can be well approximated (in terms of distance to the nth neighbor) by the Poisson point process with intensity λ_P. The smaller the λ and/or r are the better the approximation is. In our study r can be arbitrarily small. This approximation is widely used in theoretical studies, see [9] for detailed discussion.

We approach the problem as follows. Assuming isotropic propagation environment we first estimate the radius R around the tagged receiver that contains nodes creating non-negligible interference. The rest of nodes can be taken into account in the noise term N_0. The radius of the circle around the tagged receiver depends on the propagation model only. Thus, following [11] we see that using the Poisson approximation of our point pattern there are Poissonally distributed number of nodes in this circle. Furthermore, these nodes are uniformly and independently distributed in this circle.

The core of our approach is the theorem stating that for in a certain conditions the random sum of random variables tends to normal distribution [13]. In our case the summands are the distances from interferences to the tagged receiver. For sufficiently large interferers intensity λ the distribution of the power at the tagged receiver is close to the Normal. We find the parameters of this distribution directly and then use classic methods to find moments and distribution of a function of random variables to determine SINR metrics.

C. Interference

Observe that in (11) P_{R_0} is a constant value that can be estimated for any given distance d_0. The second term in the denominator of (11) is the only random term. Using the Poisson approximation of our Mattern point process we see N follows Poisson distribution with mean and variance

$$E[N] = \pi R^2 \lambda/2,\ \sigma^2[N] = \pi R^2 \lambda/2. \qquad (12)$$

For a Poisson point process, any given number of interferers in the area of radius R are independently and uniformly distributed in this area [11]. Thus, the distance to the tagged receiver, denoted as random variable D, has the same probability density function (pdf) for any i

$$f_D(d) = 2d/R^2, \qquad 0 < d < R, \qquad (13)$$

with mean $E[D] = 2/3R$ and variance $\sigma^2[D] = R^2/18$.

Consider now a random variable $G = 1/D^{-2}$. Treating the point field as a Poisson point process we see that the moments of G do not exist as

$$E[G^v] = \int_0^R \frac{2x}{R^2} \left(\frac{1}{x^{-2}}\right)^v dx \qquad (14)$$

do not converge as the integrand is unbounded approaching zero from the right. However, considering the process as Mattern hardcore one we see that the distance to the tagged receiver from any arbitrary point is lower bounded by r. For small r the deviations from the uniform distribution of interferers in a circle of radius r can be neglected. Thus, distribution of the distance to the tagged receiver could be approximated as the distance from a point arbitrarily distributed in the region bounded by two concentric circles of radii r and R, $R > r$, to their common center. It is known to be

$$f_D(d) = 2d/(R^2 - r^2), \qquad r < d < R. \qquad (15)$$

The first moment is readily computed to be

$$E[G] = \int_r^R \frac{2x}{R^2 - r^2} \frac{1}{x^{-2}} dx = \frac{\ln R - \ln r}{R^2 - r^2}. \qquad (16)$$

Similarly, the variance is

$$\sigma^2[G] = \frac{1}{2r^2 R^2} - \left(\frac{\ln R - \ln r}{R^2 - r^2}\right)^2. \qquad (17)$$

Consider now the stochastic sum of RVs G as in the second terms of the denominator of (9) and assume that the number of interferes is exactly k. With this hypothesis we have

$$E[I(\vec{d})|N = k] = P_T A_0 \sum_{i=0}^{k} E[G_i] = k P_T A_0 E[G]. \qquad (18)$$

Denoting $Pr\{N = k\} = p_k$ and unconditioning we get

$$E[I(\vec{d})] = \sum_{k=0}^{\infty} p_k k P_T A_0 E[G] = P_T A_0 E[G] E[N]. \qquad (19)$$

Now, substituting (12) and (14) into (19) we arrive at

$$E[I(\vec{d})] = \frac{P_T A_0 \pi R^2 \lambda (\ln R - \ln r)}{2(R^2 - r^2)}. \qquad (20)$$

Similarly, the second conditional raw moment is

$$E[I^2(\vec{d})|N = k] = (P_T A_0)^2 E\left[\left(\sum_{i=0}^{k} d_i^{-2}\right)^2\right] =$$

$$= (P_T A_0)^2 \sum_{i=0}^{k} \sum_{j=0}^{k} (E[G_i]E[G_j] + K_{ij}), \qquad (21)$$

where $K_{ij} = Cov(G_i, G_i)$ is the pairwise covariance.

Since G_i and G_j are pairwise independent $K_{ij} = 0$, $i = 1, 2, \ldots, M$, $i \neq j$ and $K_{ii} = \sigma^2[G_i]$, $i = 1, 2, \ldots, M$ [11].

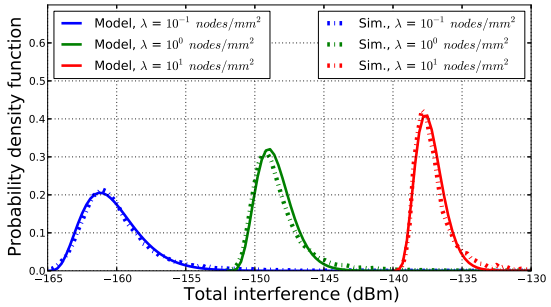

Fig. 2. Probability density function of total interference at 1THz.

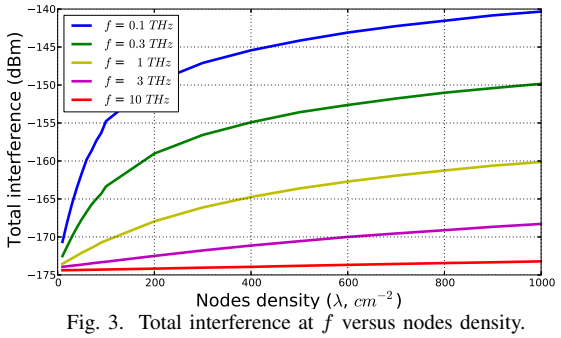

Fig. 3. Total interference at f versus nodes density.

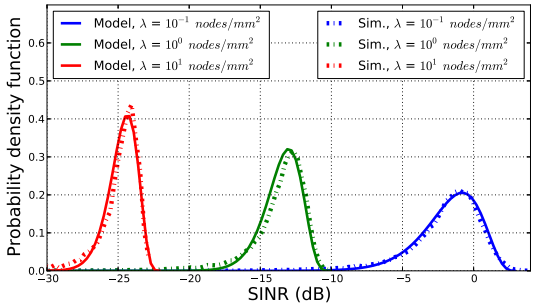

Fig. 4. Probability density function of SINR at 1THz.

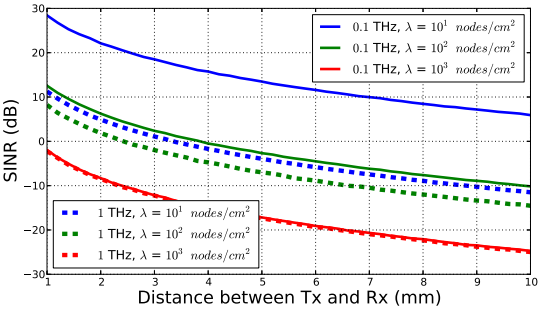

Fig. 5. SINR versus communication distance.

Further, since all G_i identically distributed $E[G_i] = E[G_j]$, $\sigma^2[G_i] = \sigma^2[G_j]$. Unconditioning (21) and applying these properties we get

$$E[I^2(\vec{d})] = (P_T A_0)^2((E[G])^2 E[N^2] + \sigma^2[G]E[N]). \quad (22)$$

The variance can now be found as

$$\sigma^2[I(\vec{d})] = P_T A_0 (E[G])^2 \sigma^2[N] + \sigma^2[G]E[N]). \quad (23)$$

D. Moments and Distribution of SINR

The moments of plain SINR does not exist as the integrals for moments does not converge similarly to (14). We will be looking for $\log_{10} S = \log S$. Denoting $\sigma^2 = \sigma^2[\vec{d}]$, $\mu = E[\vec{d}]$ and simplying the intergral for the mean we arrive at

$$E[\log S] = \log P_{R_0} - \int_{-\infty}^{\infty} N(\mu, \sigma) \log(N_0 + x)\, dx. \quad (24)$$

The integral (24) converges but cannot be expressed via elementary functions. In general for non-negative coefficients μ, σ, P_T and N_0 it is complex mixture involving Euler constant and generalized Hypergeometric function, that is, denoting the last integral in (24) by $I(\mu, \sigma, N_0)$ we have

$$I(\mu,\sigma,N_0) = \frac{1}{\log 10\sqrt{2\pi}} \sqrt{\frac{2}{\pi}} \left(-\gamma + i\pi \mathrm{Erfc}\left(\frac{\mu + N_0}{\sqrt{2}\sigma}\right) + \right.$$
$$\left. + \log\left(\frac{\sigma^2}{2}\right) + F_1^1\left(0, \frac{1}{2}, -\frac{(\mu + N_0)^2}{2\sigma^2}\right)\right), \quad (25)$$

where $\gamma \approx 0.57721567$ is Euler-Mascheroni constant, $\mathrm{Erfc}(\cdot)$ is the complementary error function, and $F_1^1(a, b, z)$ is the confluent hypergeometric function of the first kind [14]

$$F_1^1(a, b, z) = \frac{\Gamma(b)}{\Gamma(b-a)\Gamma(a)} \int_0^1 \frac{t^{a-1}(1-t)^{b-a-1}}{e^{-zt}} dt, \quad (26)$$

where $\Gamma(x)$ is gamma function.

The pdf of logarithm of SINR can be found using conventional methods of finding distributions of functions of random variables. Recall, that pdf of a random variable Y, $w(y)$, expressed as monotonous function $y = \phi(x)$ of another random variable X with pdf $f(x)$ is given by [15]

$$w(y) = f(\psi(y))|\psi'(y)|, \quad (27)$$

where $x = \psi(y) = \phi^{-1}(x)$ is the inverse function.

The inverse of $y = \phi(x) = \log(P_{R_0}/(N_0 + x))$ is unique and monotonous and given by $x = \psi(y) = 10^{-P_{R_0}} y - N_0$. The modulo of the derivative is $|\psi'(y)| = 10^{-P_{R_0}}$. Substituting these into (27), the pdf of logarithm of SINR is

$$w_{\log S}(y) = \frac{10^{-P_{R_0}}}{\sqrt{2\pi}\sigma} \exp\left(-\frac{(10^{-P_{R_0}} y - N_0 - \mu)^2}{2\sigma^2}\right), \quad (28)$$

where $\sigma^2 = \sigma^2[\vec{d}]$, $\mu = E[\vec{d}]$ being obtained in (19) and (23).

Using the same technique we can get pdf of plain SINR.

IV. Validation and Numerical Results

A. Model Validation

To validate the proposed model, we have simulated the deployment scenario, described in Section III-A. Throughout this section the considered medium is air with 1.6% of water vapor, standard pressure and temperature (10^5 Pa and 300K, respectively). Transmit power is assumed to be -10 dBm.

The critical assumption in our model is Normal distribution of interference (Lognormal in logarithmic scale). Fig. 2 shows the comparison between analytical and empirical pdfs for different λ, illustrating the interference power in dBm at 1THz. The model matches simulations well. In fact, it passes the Kolmogorov-Smirnov test with the level of significance

$\alpha = 0.05$ for all considered values of λ. Similar matching has been observed for other frequencies, distances and powers.

Fig. 4 compares pdfs of SINR for the same set of input parameters. Similarly to the interference, we see excellent matching between model and simulations. These results allow us to conclude that both the interference and SINR are very well captured by the proposed model including both moments and distribution function. Thus, in the next section, we report on qualitative and quantitative effects of interference and SINR using analytical results only.

B. Results and Discussion

Fig. 3 and Fig. 5 demonstrate the mean values of interference and SINR, respectively, for different frequencies of THz band as a function of λ with transmit power set to -10 dBm. The absorption coefficients are chosen in reverse decreasing order of the considered frequencies with $K(f)$ at 0.1 THz corresponding to almost no absorption, while $K(f)$ at 10 THz – to the most severe absorption by the medium.

Analyzing the interference data, we observe that the total level of interference expectedly grows with the nodes density. However, this growth is slower than exponential for all considered input parameters. To clarify this phenomenon, we recall that the baseline level to the provided values is the joint level of molecular noise and thermal noise that is around -174dBm. Thus, the effect of molecular noise is of secondary importance in dense THz networks compared to interference at all considered frequencies. Further, at higher frequencies the level of interference is lower for the same density of nodes λ. This is a direct consequence of path loss being proportional to the square of the frequency and absorption coefficients being usually higher as we go up in the THz band. Particularly, the level of interference at 1THz with $\lambda = 10^3$ nodes per cm^{-2} is 20 dB lower than at 0.1 THz, and, meanwhile, 14 dB higher than at 10 THz. This does not imply that SINR becomes higher with frequency as these effects negatively affect the received power of the useful signal as well.

The mean SINR in our study expectedly decreases with the distance between transmitter and receiver. Due to the presence of absorption in the path loss it depends on the operational frequency. At some frequencies it is completely dominated by the absorption with open space loss being of secondary importance (exponential versus power law functions). For example, the distance between blue and dashed-blue curves corresponding to 0.1THz and 1THz frequencies is approximately 20dB. This distance is preserved across the entire range of considered band. However, since the frequency affects the level of interference, the difference between dashed blue (1THz, $\lambda = 10$) and dashed red (1THz, $\lambda = 10^3$) lines is lower than the difference between blue and red lines (12 dB versus 30 dB).

V. Conclusions

In this paper, we have proposed an analytical model for interference and SINR approximation in dense randomly deployed THz networks. The presented model captures moments as well as distributions of both metrics. We have validated our model using simulations across a wide range of input metrics finding that it provides perfect approximations in realistic conditions. The model can be extended to the case of random distance between transmitter and receiver and more complex propagation losses, for instance, with reflection and scattering phenomena been taken into account.

Due to limited space, we presented only basic trade-offs between input parameters reporting only the most interesting phenomena. The secondary importance of the molecular noise is one of them. Further, even the thermal noise does not play substantial role in the interference process. This is partially explained by the dense scenario we targeted but cannot be fully attributed to it. Even when the density of nodes is lower, interference is the major term in the denominator of SINR affecting the resulting value. The consequence is possibility to neglect these terms when assessing coverage and rate performance of THz networks and apply techniques developed so far for dimensioning of lower frequency networks.

Acknowledgment

This work was supported by Academy of Finland FiDiPro program "Nanocommunication Networks", 2012 – 2016.

References

[1] M. Jornet and M. Akyildiz, "Channel modeling and capacity analysis for electromagnetic wireless nanonetworks in the terahertz band," *IEEE Trans. Wir. Comm.*, vol. 10, pp. 3211–3221, Oct. 2011.

[2] P. Boronin, V. Petrov, D. Moltchanov, Y. Koucheryavy, and J. Jornet, "Capacity and throughput analysis of nanoscale machine communication through transparency windows in the terahertz band," *Elsevier Nano Communication Networks*, vol. 5, pp. 72–82, Sept. 2014.

[3] Y. Yang, M. Mandehgar, and D. Grischkowsky, "Understanding of THz pulse propagation in the atmosphere," *IEEE Trans. THz Science Tech.*, vol. 2, pp. 406–415, July 2012.

[4] I. Akyildiz, J. Jornet, and M. Pierobon, "Nanonetworks: A new frontier in communications," *Comm. ACM*, vol. 54, pp. 84–89, Nov. 2011.

[5] J. Jornet and I. Akyldiz, "Femtosecond-long pulse-based modulation for terahertz band communication in nanonetworks," *IEEE Trans. Comm.*, vol. 62, pp. 1742–1754, May 2014.

[6] www.cfa.harvard.edu, "Hitran: High-resolution transmission molecular absorption database," tech. rep., Harvard-Smithson Center for Astrophysics, 2014.

[7] N. Atindra and A. Ghosh, "Ultralow noise field-effect transistor from multilayer graphene," *Appl. Phys. Let.*, vol. 95, no. 8, pp. 103–106, 2009.

[8] L. Kish, "Stealth communication: Zero-power classical communication, zero-quantum quantum communication and environmental-noise communication," *Appl. Phys. Let.*, vol. 87, 2005.

[9] H. ElSawy, E. Hossain, and M. Haenggi, "Stochastic geometry for modeling, analysis, and design of multi-tier and cognitive cellular wireless networks: A survey," *IEEE Comm. Sur. Tut.*, vol. 15, pp. 996–1019, July 2013.

[10] F. Baccelli and B. Blaszczyszyn, *Stochastic Geometry and Wireless Networks, Part I: Theory*. Now Publishers, 2009.

[11] S. Chiu, D. Stoyan, W. Kendall, and J. Mecke, *Stochastic geometry and its applications*. Wiley, 2013.

[12] D. Moltchanov, "Distance distributions in random networks," *Elsevier Ad Hoc Networks*, vol. 10, pp. 1146–1166, Aug. 2012.

[13] A. Pecinkin, "On convergence of random sums of random variables to the normal law," *Teor. Ver. Prim.*, vol. 18, no. 2, pp. 380–382, 1973.

[14] M. Abramowitz and I. Stegun, *Handbook of Mathematical Functions with Formulas, Graphs, and Mathematical Tables*. Dover, 1965.

[15] W. Feller, *An introduction to probability theory and its applications*, vol. 1. Wiley, 3rd ed., 1968.